

DARLINGTON N12 INVESTIGATION
MODELLING OF FUEL BUNDLE MOVEMENT IN CHANNEL UNDER PRESSURE
PULSING CONDITIONS

J.H.K. Lau, M. Tayal*, E. Nadeau, M.J. Pettigrew**, I.E. Oldaker*,
W. Teper, B. Wong*, F. Iglesias

Ontario Hydro
700 University Avenue
Toronto, Ontario
Canada, M5G 1X6

ABSTRACT

Activities in fuel and fuel string modelling were undertaken as a part of the overall program to determine the cause of fuel damage in Darlington Units 1 and 2. The aim is to establish the fuel response in a fuel channel under loading and pressure pulsing conditions. This paper provides an overview of these modelling activities, and present sample results to illustrate the fuel response trends.

1.0 INTRODUCTION

As a part of the Darlington N12 investigation, a program to model the fuel and fuel string behaviour that may lead to the fuel damage was initiated. This program evolved over time, guided by results from fuel inspections, post-irradiation examinations, metallurgical examinations and loop testing.

When endplate cracks were first identified in Unit 2, the assessment was initially focused on the static load on the fuel bundles in the channel, and the resultant stresses on the endplates of the latch bundle (bundle 1). The latch bundle supports the hydraulic drag load of 12 upstream bundles. This hydraulic load is dependent on the coolant flow rate and is approximately proportional to the mass flow squared. Since bundle 1 is, in turn, supported by the latch on only 14 outer elements, the stresses on the endplates are dictated by how the loads from the upstream bundles are transferred to the inner and outer elements of the latch bundle. The load shedding, stack load on bundle 1, and endplate stress distribution were assessed (References 1, 2 and 3). The results showed that the observed endplate cracks in Darlington Unit 2 latch bundles are generally at the locations of high predicted stresses.

* AECL-CANDU

** AECL-Chalk River Laboratories

When the metallurgical examination of the endplate cracks demonstrated that the damage is due to fatigue, possibly because of flow variations or pressure pulsing, bundle vibration characteristics were investigated. Tests were performed on a shaker table at Ontario Hydro Research Division (OHRD) to look at the transverse and axial movements of elements, and to see whether this would cause endplate cracks (Reference 4). Modelling work has also been performed to predict the different bundle vibration modes and their natural frequencies (Reference 5). The work demonstrated that the vibration characteristics of the fuel elements are non-linear, and that the transverse and axial vibrations of the elements are coupled and can result in endplate cracking.

Metallurgical examination of bearing pads on bundles from Darlington and the pressure tube wear surfaces have shown axial as well as some transverse scratches, which suggests that the predominant motions of the outer fuel elements are axial in direction. Testing at Unit 1 and Unit 2 indicated acoustic resonance in the heat transport system which led to pressure pulses in the channel predominantly at 150 Hz frequency. Loop tests at STERN Laboratories have demonstrated that pressure pulses can cause fatigue cracking of the endplates. The loop test data also suggested that mechanical resonance of the fuel string could result in endplate cracking at lower pressure pulse amplitudes than if the fuel string is not in mechanical resonance. The fuel string natural frequencies depend on the axial stiffness of the bundles, and these are expected to change during irradiation. All of these factors indicated that fuel damage would be a result of axial vibration of the fuel string, under hydraulic load and pressure pulsing conditions. Also, mechanical resonance of the fuel string (i.e, when the natural frequency matches the pressure pulse frequency) may be an important parameter in the fuel response in Unit 1 and Unit 2. The coupling of the transverse and axial element movements, as observed in the earlier shaker table tests, explains the observation that some of the wear on inter-element spacer pads as well as pressure tube may result from transverse motion of the fuel elements, apart from the axial motion.

As a result of these findings, the focus was shifted to model the axial response of a 13 bundle fuel string. A fuel & fuel string modelling team was formed, consisting of the authors of this paper, to carry out the activities. Modelling is performed for unirradiated bundles, in order to compare to the loop test data to facilitate data interpretation. Fuel bundles under power operation are also modelled, in order to simulate the response during Unit 1 and Unit 2 operation.

Since the axial response of the fuel string depends on the axial stiffness of individual fuel bundles, one of the activities is to model the axial stiffness of unirradiated fuel bundles as well as fuel bundles during power operation. Another activity is to

develop an uniaxial fuel string model to simulate the axial vibration of the fuel bundles in a channel under hydraulic load and pressure pulsing conditions. Apart from the development of methodology and models, laboratory tests to provide data for model input and validation are also performed. Figure 1 summarizes the activities involved. Some of the activities have been completed, while others are still ongoing. This paper provides an overview of the work, and presents sample results to illustrate the trends in fuel response. However, due to the ongoing nature, some of the most recent analyses were not ready in time for inclusion in this paper. Nevertheless, the overall results and the conclusions remain unchanged.

2.0 AXIAL STIFFNESS OF FUEL BUNDLES

2.1 Unirradiated Bundles

For modelling bundle stiffness, a number of effects as schematically shown in Figure 2 are considered. These include: axial stiffness of the fuel elements (sheaths and pellets), bending/bowing of the fuel elements, parallelogramming of the bundle, and the end plate waviness.

(i) Sheath Compression

The axial compression of the sheath refers to the shortening of the length of an individual fuel sheath under a compressive load. The parameters that govern sheath compression are the Young's modulus of the sheath, the cross-section area of the sheath, and the length of the sheath.

(ii) Pellet Compression

The pellets can also contribute to the stiffness of the fuel element if there is a tight circumferential or axial contact between the pellets and the sheath and endcaps. In unirradiated fuel elements, the pellets and the sheath are separated by axial and diametral clearances, hence, the pellet does not participate in the axial stiffness.

(iii) Element Bending/Bowing

Fuel elements exhibit a certain degree of lateral bending due to as-manufactured bows, and circumferential temperature gradients when the fuel is at power in the reactor.

An axial force will increase the bow which, in turn, will decrease the axial length. This is another source for element compliance. The governing parameters are element flexural rigidity, element length, and the magnitude of bow. However, for a fuel bundle in a fuel channel, the degree of lateral movement is small as the fuel elements are constrained by the bearing pads

and inter-element spacers. Therefore, this tends not to be an important contribution to the compliance, as confirmed by the bundle compression tests.

(iv) Parallelogramming

Within manufacturing tolerances, a small degree of "parallelogramming" may exist in the as-fabricated bundles. This means that the endplates are not perfectly square to the longitudinal axis of the bundle. This can be removed under a very small applied load. Under the high hydraulic loads in a fuel channel, this effect is not significant.

(v) Endplate Compliance

As-fabricated bundles have "wavy" end plates due to two reasons:

- (1) Welding of the elements to the endplates leads to local deformation, termed "small" waves, in the webs between two adjacent elements.
- (2) The welding process also results in some deformation of the endcaps/spigot. This causes different element lengths when measured from endplate to endplate. It forms the "large" waves on the endplate.

Figure 3 shows an example of the endplate waves measured on production fuel bundles. The small waves are about 0.06 mm high, with a maximum of approximately 0.07 mm. The height of the big waves varies between elements. Generally, the overall differential in element lengths between the outer and inner elements is a maximum of about 0.2 mm for fuel bundles manufactured by GE Canada, and a maximum of 0.6 mm for bundles manufactured by Zircotec Industries.

For each of the components of bundle compliance, equations for load versus deflection are formulated using standard principles of classical mechanics. The spring constants of the components are then summed in an appropriate manner (i.e., some springs in series; others in parallel) to calculate the overall spring constant of a fuel bundle. When two or more components are connected in series (e.g., the sheath and the endplate), then the most compliant component dominates the overall behaviour. When the components are connected in parallel (eg., the different fuel elements within a ring of elements), the stiffest component dominates the overall behaviour.

To provide the test data to validate the method of calculating bundle stiffness, axial compression tests of fuel bundles were conducted at the INSTRON load frame in the Metallurgy Laboratory at Sheridan Park Engineering Laboratories (SPEL). Fuel bundles were axially compressed and the corresponding loads and deflections measured. Two support systems for the bundle were

used: two flat plates, one at each bundle end, for distributed load measurement, and two rings, one at each bundle end, for outer element load measurement. Single and two bundle compression tests were performed with GEC as well as ZIRCATEC bundles. Tests were performed with unclamped bundles and with bundles clamped at the mid-plane to study the effect of element bow on the axial stiffness.

The test results confirm our understanding of fuel bundle stiffness and its different components. The results also confirm the validity of the model in predicting the axial stiffness. Figure 4 compares the measurements to the calculations for ZIRCATEC and for GEC bundles respectively for outer-element loading. The first region of the curve represents the removal of parallelogramming. The second region represents the load range at which the "large" waves (i.e., those created by the variations in element lengths) are flattened. As noted earlier, the length-variations are larger in the ZIRCATEC bundle than in the GEC bundle. Thus the ZIRCATEC bundle requires a larger load to remove the big waves. By the end of the second region, the elements have been compressed sufficiently so that, within the ring, they are now equal in length. In the third region, the compliance represents contributions from all the 18 outer elements as well as from the "small" waves in the end plates. In general, the calculations show a reasonable agreement with the measurements.

To provide further data to validate the bundle stiffness calculation, compression tests on single elements with endplates attached at their ends were also performed in the INSTRON load frame. Each element tested was obtained from a fuel bundle by cutting the endplate web at its mid-points between neighbouring elements. The results of the single element compression tests also compared well with predictions.

2.3 Fuel Bundles During Power Operation

Unlike unirradiated fuel, the radial and/or axial gap in fuel elements during power operation may be closed due to various physical processes. Thus, the axial stiffness is dependent on the (radial) interfacial pressure between the sheath and the UO_2 pellets, and the presence or absence of an axial gap in the fuel element. In the absence of an axial gap, both the sheath and pellets act together as a single structure, and the resulting axial stiffness is high compared to that of the sheath alone. Even when there is an axial gap, if the interfacial pressure is high, axial load will still be transmitted to the pellets, providing a high stiffness. The stiffness reduces to that of the sheath only when there is an axial gap coincident with a low interfacial pressure.

The axial gap and the interfacial pressure during irradiation are governed by various physical processes. Generally, thermal expansion resulting from power increases, fission product swelling of UO_2 , and sheath creep are the processes which increase the interfacial pressure or close the axial gaps. The processes which decrease the interfacial pressure or open the axial gaps are thermal contraction resulting from power reductions, UO_2 densification, and sheath stress relaxation. This complicated inter-relationship of the various processes and the effects on the interfacial pressure and axial gap of fuel elements during irradiation were assessed with the fuel performance code ELESTRES (Reference 6) and the structural code BEAM. The power burnup histories calculated by fuel management codes were used as input.

To-date, there is no direct measurement of the axial stiffness of fuel elements during on-power operation. At power, a fuel pellet consists of a hot plastic UO_2 core, and an outer peripheral region which has cracks normal to the axis. The axial stiffness of the pellets depends on the size, number and distribution of these cracks which are subject to large uncertainties. Therefore, when the ELESTRES/BEAM codes predict that the pellets contribute fully to the axial stiffness, either because the axial gap is closed, or the interfacial pressure is high, a lower and upper range of stiffness values for the combined structure were assumed. The lower range assumes that the entire pellet stack is cracked. The Young's modulus of cracked pellets were measured in tests performed at Chalk River Laboratories (CRL). In the tests, the endcaps of irradiated Darlington fuel elements were removed, and the load deflection curve of the irradiated cracked pellets was measured in the hot cell. Since the elements were discharged from the reactor, cooling will produce distributed cracks within the pellets. This lower range value is a factor of about 3.5 times the stiffness of the sheath alone. The upper range of stiffness assumes that the pellets are not cracked, and the Young's modulus of solid UO_2 was used. This yields an axial stiffness of the fuel element which is a factor of 14 times the sheath axial stiffness.

As an illustration, Figure 5 shows the calculated axial stiffness of an outer element in Bundles 1, 3, 7 and 10 in Unit 2 Channel K13 where endplate cracks have occurred. The results show the following trends:

- (i) At cold ($20^\circ C$), unpressurized and unirradiated conditions, the axial stiffness of a fuel element is that of an empty sheath and is approximately equal to 3.2 MN/m.
- (ii) Under pressurized (10.7 MPa), hot ($290^\circ C$) and high-power conditions, the UO_2 pellets participate fully in stiffening the fuel element. The axial stiffness

increases by a factor of about 14, to approximately 47 MN/m (upper-range estimate).

- (iii) In bundle positions 3 and 10, the axial stiffness is calculated to drop at around 1500-1600 hours after startup due to UO₂ densification, and then returns to its high value at about 1700 hours. The drop in stiffness occurs when both the axial and the radial gaps are open. This condition occurs when pellet contraction due to densification is faster than the inward creep of the sheath. Once sheath creep closes the axial and/or the radial gap, the axial stiffness returns to a high value.
- (iv) In bundle positions 1 and 7, high axial stiffness (about 47 MN/m) is maintained up to refuelling (about 3200 hours). This is due to one of the following:
 - (1) the axial gap is open but there is sufficient interfacial pressure to maintain high stiffness (position 1); or
 - (2) the timing of axial gap opening and radial gap opening do not coincide (position 7).
- (v) In general, the outer element axial stiffness decreases following a large reduction in power (e.g., the 35% power drop at approximately 3500 hours) (positions 1, 7 and 10). However, the axial stiffness may increase again if creep of the sheath onto the pellet closes the gaps.
- (vi) In position 3, the stiffness does not decrease with the 35% power drop at about 3500 hours, since the thermal contraction due to the power drop is insufficient to open the gaps.

The results demonstrate that the axial stiffness of a 13 bundle fuel string tends to increase as the Unit 2 reactor reached full power. The stiffness decreased temporarily at about 1500 hours due to densification. The stiffness also decreased when there was a large power reduction.

In addition to the change in fuel element stiffness, power operation also changes the compliance of the endplate. There are three effects:

- (i) stiffening due to pellet expansion;
- (ii) creep of the fuel element; and
- (iii) creep of the endplate

When the fuel is raised to full power, thermal expansion of the pellets stiffens the fuel elements. By itself, this tends to

increase the stiffness of the bundle. However, the situation is modified when the effect of large endplate waves (i.e., length equalization) is also considered. Compared to the off-power situation, a given hydraulic load leads to less on-power deflections of the individual stiffened fuel elements. This in turn leads to a smaller equalization of element lengths. Thus, a smaller number of fuel elements share the axial load. This counteracts the increased stiffness of the individual elements. The net effect represents a balance between the increased stiffness of the individual fuel elements versus the decreased number of elements sharing the load (i.e., less initial flattening of the large waves by the hydraulic load).

The hydraulic load introduces compressive axial stresses on the endplates. Combined with the elevated temperatures and the high neutron flux, this leads to axial creep, which reduces the waviness of the endplate. Flatter endplates are less compliant. Thus, the endplate stiffness is expected to increase with irradiation time. Preliminary results indicate that at locations not already flattened by elastic compression, many months are needed to cause additional flattening via creep.

The methodology and models previously described are used to assess the stiffness of the fuel string under different operating conditions. These stiffness values are then used in the fuel string model to assess the fuel string natural frequency and fuel string response.

3.0 UNIAXIAL FUEL STRING MODEL

An uniaxial model of the fuel string was developed in order to assess the overall behaviour of the thirteen fuel bundles in a fuel channel (Reference 5). Each fuel bundle is modelled using four masses joined by four springs as shown in Figure 6. This simple one-dimensional bundle model divides the bundle into two structural parts: the 18 fuel elements in the outer ring, and the 19 inner fuel elements that consist of the central element and the elements in the intermediate and inner rings. The mass of the 18 outer elements is simulated using 2 masses labelled M1, each of them having the mass of 9 fuel elements. The combined axial stiffness of the 18 outer elements and their associated endplate waves are represented by the spring stiffness K1. Similarly for the inner fuel elements, M2 has a mass of 9.5 elements and the stiffness K2 represents the combined axial stiffness of the 19 inner elements and their associated endplate waves. The inner and outer parts of the bundles are joined by a pair of springs K3 which represent the compliance of the radial ribs of the endplates.

Thirteen basic fuel bundle units are assembled to form the fuel string shown in Figure 6. Mass M3 and spring K4 represent the

mass and the stiffness of the shield plug and liner tube (end-assembly) of the fuel channel respectively.

The values of K1 and K2 are predicted with the methodology discussed in Section 2.0. They are a function of the applied hydraulic load. The value of K3 is obtained by tuning a single uniaxial bundle unit to the first axial bundle mode (78 Hz) found experimentally at SPEL. This corresponds to $K3 = 1.385 \text{ MN/m}$. M3 and K4 are evaluated based on the geometry and material properties of the channel end assembly.

For modal analysis, stiff spring elements (K5) are used to connect the contact surfaces from bundle to bundle. It is assumed that the endplates of the bundles are flat, (i.e. that there are no gaps between the bundles at the centre line). The contact between bundle 1 outer elements and the end-assembly (i.e., between node #1 and node #53) is also modelled using a stiff spring, which reproduces the latch support conditions. The fuel string model consists of 54 nodes and 78 spring elements. Only axial motion is allowed.

For dynamic analyses, K1, K2 and K5 springs are replaced by non linear analog elements. The advantage of the non-linear analog elements is that their behaviour can be represented by the entire load-deflection curve instead of a fixed distinct value. Also, the inter-bundle springs K5 are modelled as gap elements which can take compression forces but no tension. This allows the fuel string to separate if the alternating forces are large enough to overcome the hydraulic drag load.

3.1 Comparisons to Experiments

Frequency sweep tests were performed at the STERN loop with 13 GEC bundles at a temperature of 59 C with a channel flow of 31.4 kg/s. Peak response of the endplate deflection for the latch bundle was observed at various frequencies during the sweep. These frequencies of peak response likely correspond to the natural frequencies of the fuel string. Modal analysis of the fuel string was performed with the uniaxial fuel string model for the conditions of the STERN loop test. The calculated natural frequencies of the fuel string are compared to the observed frequencies of peak response in Table 1.

Due to its simplicity, the fuel string model will not yield all the natural frequencies that were observed in the test. Also, some of the peak responses in the test may be due to a loop acoustic effect, and may not be due to fuel string resonance. Nevertheless, agreement between model predictions and experimental results is good.

The analytical mode shapes are plotted in Figures 7a and 7b for Mode 4 and Mode 5 respectively. The natural frequencies for

Mode 4 is 121 Hz and Mode 5 is 139 Hz. These are close to 150 Hz, which is the frequency of the dominant pressure pulse measured in the heat transport system at Darlington NGS. Each mode shape is represented by two graphs, showing the normalized displacements of the outer fuel elements and the inner elements respectively.

3.2 Results of Fuel String Calculations

To illustrate the dynamic response of the fuel string, simulation results are presented for a GEC fuel string at Mode 5 (natural frequency of 139 Hz), excited by a 139 Hz pressure wave. In the simulation, a drag load of 691 N (Reference 2) is applied on each bundle. It is assumed that the pressure pulse is generated by a standing wave in the channel, with an amplitude of 10 psi zero to peak, a wavelength of about 5.4 m, and an antinode at the upstream end of bundle 13. It is also assumed that the pressure is uniformly distributed on the cross-sectional area of all 37 fuel elements.

In the simulations, the drag load is applied first, using a ramp function from time $t_1=0.0$ s to $t_2=0.1$ s. The system is allowed to reach a steady state condition resulting from the application of the drag load before the pulsating load is applied. This latter load is applied using a ramping function from time $t_3=0.2$ s to $t_4=0.25$ s. It is assumed that the damping is 1% and that the friction forces between the bundles and the pressure tube are negligible.

Figure 8 shows the bundle 1 nodal displacements. The drag load causes doming of the endplates towards the channel outlet. The predicted static deflection of the bundle 1 downstream endplate is on the order of 0.8 mm. This is caused by the stack load of 8983 N (691 N/bundle). This drag load corresponds to a flow rate of approximately 34 kg/s under cold conditions. The deflection of the bundle 1 downstream endplate was measured as a function of mass flow rate at OHRD for a string of GEC fuel under cold conditions. The data indicates that at about 34 kg/s mass flow, the endplate deflection is about 0.7 mm. Thus, there is good agreement between model prediction and measurement. Note that the pulsating load is applied using a ramping function from time 0.2 s to 0.25 s. As shown in Figure 8, after 0.3 seconds of running time, the steady response of the system is attained.

Figure 9a plots the maximum amplitude of vibration in the steady-state regime for the inner and outer elements axially along the channel. Figure 9b plots the relative amplitude of vibration between the inner and outer elements. It can be seen that the amplitude of relative vibration between the inner and outer fuel elements is highest at bundle 1. This factor, combined with the high mean stress due to the hydraulic load, is consistent with the observation that bundle 1 endplates are most

susceptible to fatigue cracking, as found in Darlington Unit 2 for GEC fuel string. Also, the amplitude plot indicates that the outer elements of bundle 13 have the highest amplitude of vibration. This may also explain the high bearing pad and pressure tube fretting wear observed in Darlington Unit 2 at the bundle 13 location.

3.3 Fuel String Natural Frequency During Darlington Unit 2 Power Operation - Sensitivity Studies

Various scenarios of fuel string stiffness were postulated to provide a qualitative trend of how fuel string stiffness might change during reactor operation. The natural frequencies of the fuel string were evaluated for these scenarios using the uniaxial fuel string model. Since the frequency of the dominant pressure pulses measured in Darlington reactors is 150 Hz, the resonance modes that have frequencies close to 150 Hz were examined in more detail. These are Modes 4, 5 and 6. Figure 10 summarizes schematically the calculated natural frequencies of the fuel string in Mode 4, 5, and 6 for the various scenarios.

As indicated for each scenario, two cases are considered: (i) the upper bound fuel element axial stiffness which is a factor of 14 greater than the unirradiated value, and (ii) the lower range stiffness which is a factor of 3.5 greater. As discussed in Section 2.1, this range of stiffness reflects the uncertainties related to the pellet crack size, number and distribution at power.

Scenario 1 represents the fuel at cold, unirradiated conditions (20°C). Scenario 2 represents full power operation with full endplate compliance (i.e., before any endplate waviness is removed by creep). It can be seen that even when the fuel element stiffness is assumed to be increased by a factor of 14 from its unirradiated value, the natural frequencies of the three modes are not drastically increased. This is due to the endplate compliance. They represent soft springs and they tend to dominate the overall fuel string stiffness.

Scenario 3 represents the situation when UO₂ densifies. Densification causes the fuel element stiffness to drop. This causes the reduction of the natural frequencies from those in scenario 2.

Scenario 4 represents the situation of full power operation for a long period where portions of the endplate compliance would have been removed by creep. Thus, the fuel string stiffness increases, which results in an increase in the natural frequencies.

Scenario 5 represents a drop in the reactor power of 35% or more. This causes pellet contraction and reduces the element stiffness. The natural frequencies reduce from those in scenario 4.

As shown in Figure 10, upon startup of the Darlington reactor, the natural frequencies increase from the zero power situation. Densification, which occurs early (estimated to be completed by 1500 hours for Unit 2) will lower the frequency, as will a large power drop. However, as time proceeds, the creep of the endplate will tend to increase the fuel string natural frequencies. Mode 5 is the most likely to move to a frequency of 150 Hz. Mode 4 also has the potential to move to 150 Hz, but only for the cases involving the upper range in the uncertainty of the axial stiffness estimates. It can be seen from this trend analysis that it is possible that, during power operation, the fuel string can have a natural frequency of 150 Hz. This is due to the large number of possible fuel string vibration modes, and the stiffening of the fuel string during power operation.

4.0 RECENT DEVELOPMENTS

Due to the ongoing nature of the investigation, the results and methodology presented in this paper do not always reflect the most current status. Improvements have been made on the fuel string model, such as separately representing the stiffness of the endplates and that of the fuel elements, the modelling of friction between the bundles and the pressure tube, and the validation of the fuel string prediction with preliminary test data recently obtained. In addition, the stiffness calculations have been improved, accounting for temperature and pressure changes along the fuel channel. Furthermore, a structural model consisting of a solid UO_2 core, a severely cracked peripheral region, and a sheath has recently been developed to predict the axial stiffness of a fuel element at power when the fuel pellets are in good contact with the sheath. The model agrees well with the flexural rigidity results of the CRL U118 tests (Reference 7). This model provides a maximum stiffness value of the fuel element at 8.5 times the sheath stiffness, which is between the lower and upper range values assumed in the sensitivity studies presented in this paper. All of these revisions, however, do not substantially alter the response trend and the overall findings.

5.0 SUMMARY OF FINDINGS TO-DATE

A large number of analyses have been performed with the previously discussed models and methods to elucidate the fuel and fuel string response in Unit 1 and Unit 2 under pressure pulsing conditions. The overall findings to-date are as follow:

- (i) The fuel string has a large number of axial vibration modes. The number of modes is likely

larger than that predicted, since the simple lumped parameter uniaxial fuel string model cannot capture all the possible modes.

- (ii) The fuel string stiffness consists of the stiffness of the fuel elements and of the endplates. Upon initial startup of Unit 2, the element stiffness is predicted to increase rapidly since thermal expansion causes the pellet to interact with the sheath. Element stiffness is reduced upon UO_2 densification, which occurred for the Unit 2 power history at about 1500 hours from startup. About 200 hours later, the stiffness is predicted to increase to the previous value. Element stiffness is predicted to decrease if there is a significant power drop, such as in a 35 % reactor power reduction, or during fuelling when high power bundles are shifted into the position of lower bundle power. The natural frequency of the fuel string increases with the stiffness.
- (iii) Endplate waviness/compliance, representing a softer spring than the fuel element, moderates the increase in the fuel string stiffness from fuel element stiffening. However, endplate compliance will be removed by Zircaloy creep during irradiation. The creep rate is expected to be higher for downstream bundles due to the higher hydraulic load.
- (iv) Mode 5 is the likely mode in which fuel strings responded to the 150 Hz pressure pulses in Unit 2, leading to the observed fuel damage.
- (v) It is possible that the fuel string natural frequency (Mode 5) would change during Unit 2 power operation, to coincide with the frequency of the dominant pressure pulses (150 Hz) measured in the reactors. This would lead to resonance response of the fuel string. However, because of the non-linearity of the fuel bundles, it does not appear that the difference between resonance and off-resonance response is large. Thus, the fuel string response is likely dominated by the acoustic pressure wave in the fuel channel.

6.0 REFERENCES

- (1) GVILDYS, P., "Fuel Bundle Endplate - Preliminary Stress Analysis", CGE Report R91CAP1 Rev 0.
- (2) HO, S., "13 Bundle Model - Stack Load on Bundle 1", Ontario Hydro Design Calculation 37000-8, May 17, 1991.

- (3) STRZELCZYK, A., "Stresses at Endplates of Fuel Bundle", Ontario Hydro Design Calculation 37000-1, April 5, 1991.
- (4) BLACK, D.A. and D'ANGELO, J.P., "Vibration Testing of Fuel Bundles - Interim Report", OHRD Report No. 91-272-H, December 19, 1991.
- (5) NADEAU, E., "Dynamic Simulation of Darlington NGS Fuel", OHRD Report No. 92-53-K, February 1992.
- (6) TAYAL, M., "Modelling of CANDU Fuel Under Normal Operating Conditions: ELESTRES Code Description", AECL Report AECL-9331, 1987.
- (7) PETTIGREW, M.J., and Turner R.B., "The In-Reactor Vibration Behaviour of CANDU Fuel", Paper No. 1e, Presented at a Seminar on Vibration of Reactor Fuel and Steam Generator Tubes, Moscow, September 9-12, 1975, organized by the USSR State Committee for the Use of Atomic Energy and Atomic Energy of Canada Limited.

ACKNOWLEDGEMENT

We like to acknowledge M. Gabbani (AECL-CANDU) for his contribution in the bundle compression tests, R. Mak (AECL-CANDU) for modelling endplate creep, Bruce Smith (AECL-CRL) for his contribution in the stiffness tests on irradiated fuel, and J. DeVaal (AECL-CRL) for calculating the axial stiffness of cracked pellets.

Table 1
Comparison of Calculated Fuel String Natural Frequencies to the
Frequencies of Peak Endplate Response Observed in STERN Loop
Sweep Tests

| ANALYTICAL | | EXPERIMENTAL |
|------------|--------|----------------|
| MODE | f (Hz) | |
| 1 | 26.5 | 14 31 60 |
| 2 | 73.2 | 75 |
| 3 | 112.4 | 105 |
| 4 | 120.6 | 120 |
| 5 | 139.4 | 138 |
| 6 | 165.5 | 146 164 |
| 7 | 181.4 | 178 |
| 8 | 203.0 | |
| 9 | 219.8 | |
| 10 | 241.6 | |

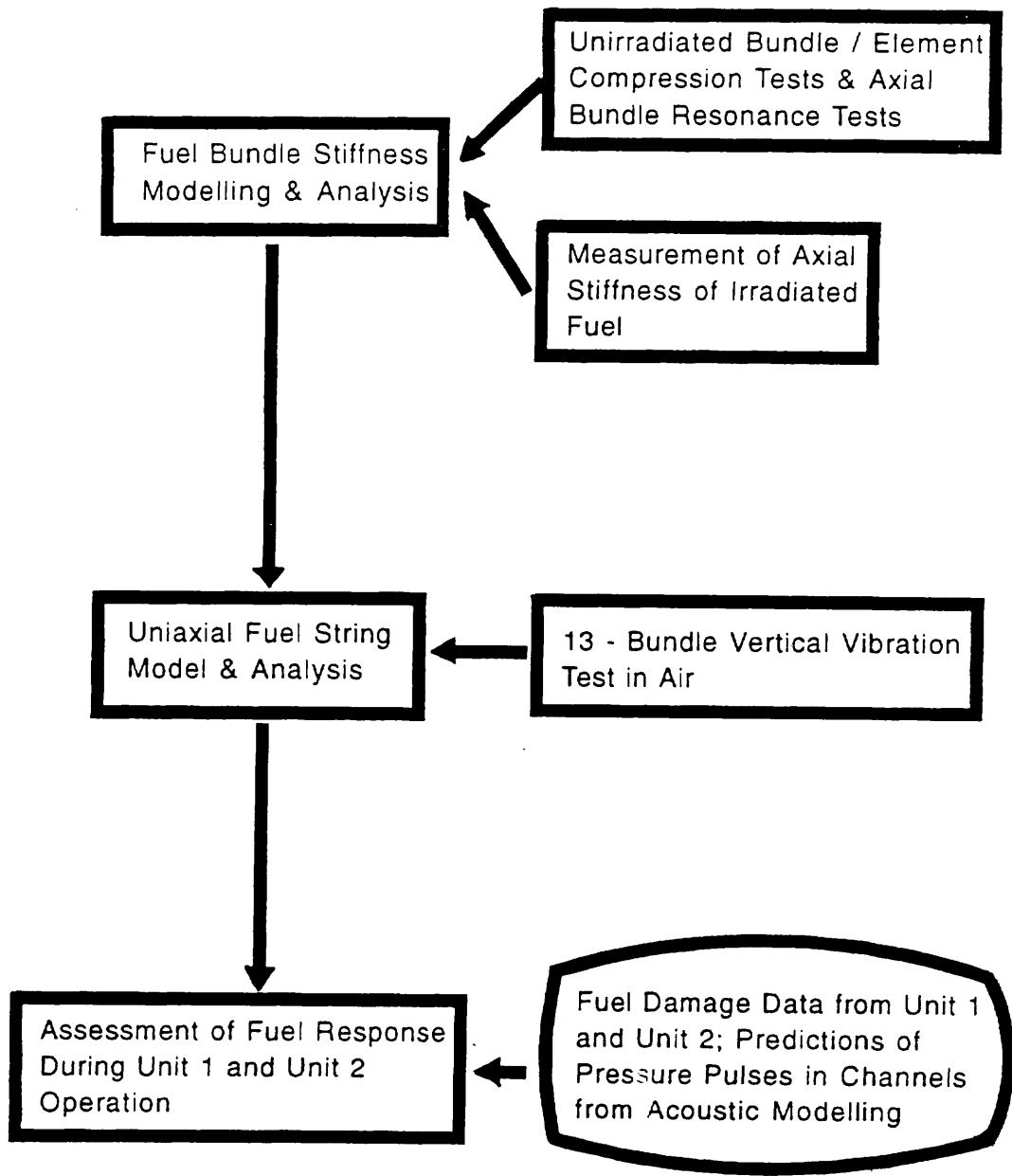
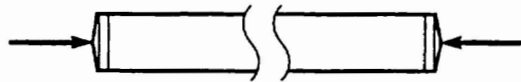
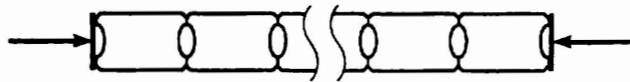


Figure 1

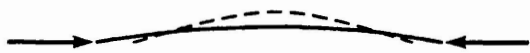
**Program Outline - Modelling Axial Response of
Fuel String Under Pressure Pulsing Condition**



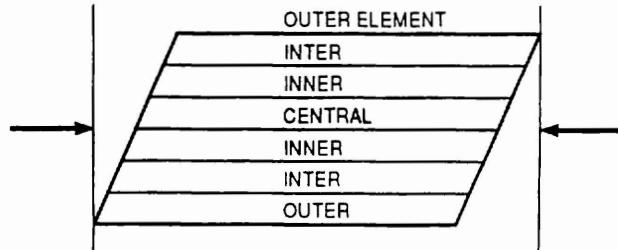
SHEATH COMPRESSION



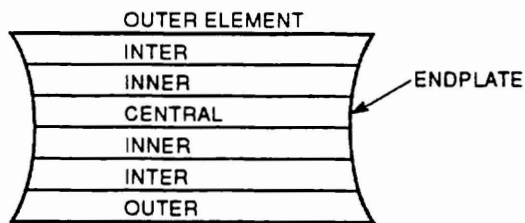
PELLET COMPRESSION



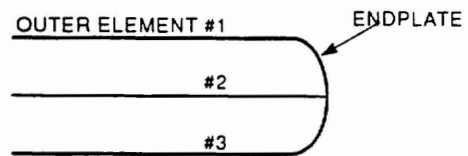
ELEMENT BENDING



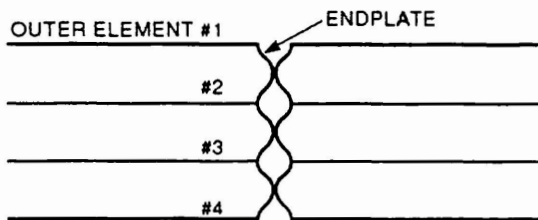
BUNDLE PARALLELOGRAMMING



BIG WAVE: RADIAL



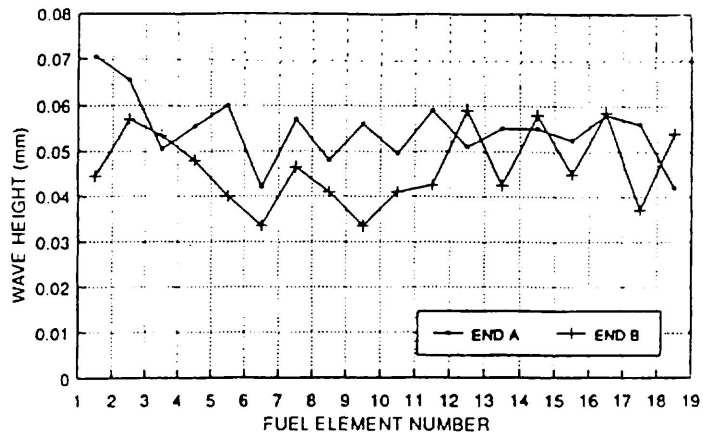
BIG WAVE: CIRCUMFERENTIAL



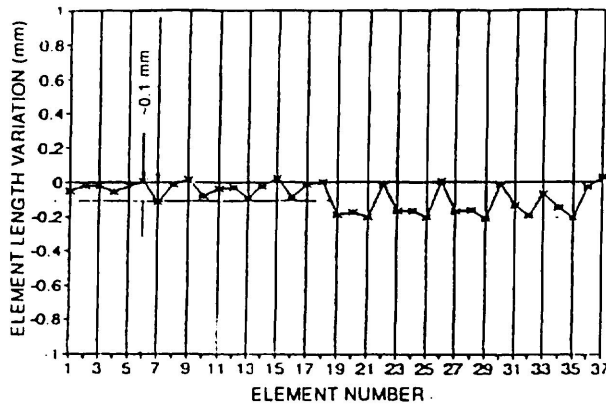
SMALL WAVE

NOTE:
FOR CLARITY THE DISTORTIONS
AND THE WAVES HAVE BEEN
EXAGGERATED

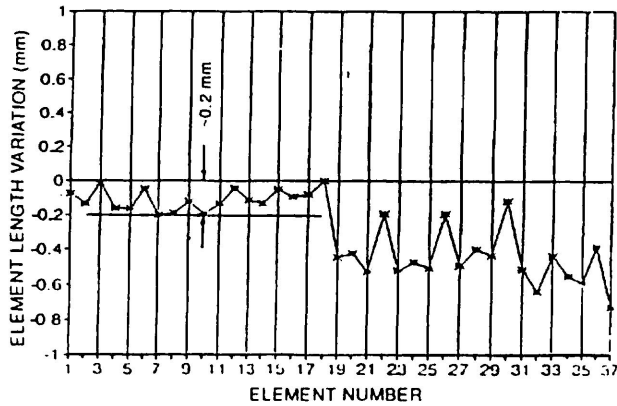
FIGURE 2
COMPONENTS OF BUNDLE COMPLIANCE



(A) SMALL WAVES: GEC BUNDLE



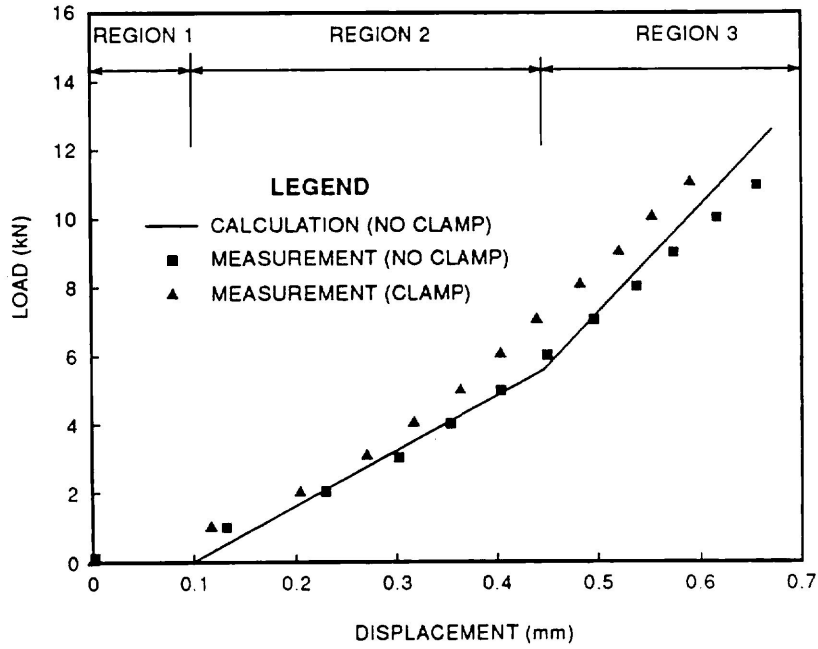
(B) BIG WAVES: GEC BUNDLE



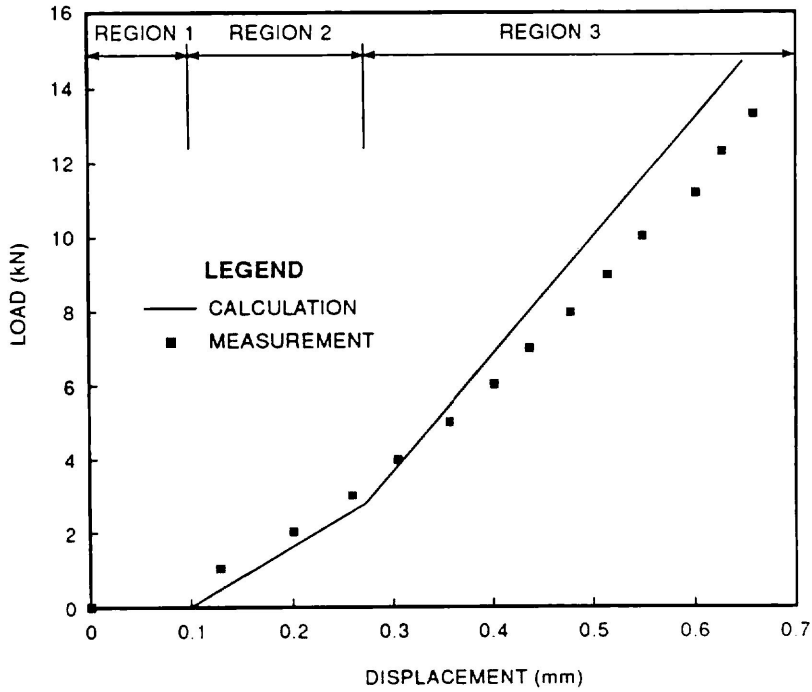
(C) BIG WAVES: ZIRCATEC BUNDLE

| RING | ELEMENT NUMBERS |
|--------------|-----------------|
| OUTER | 1-18 |
| INTERMEDIATE | 19-30 |
| INNER | 31-36 |
| CENTRAL | 37 |

FIGURE 3
ENDPLATE WAVES



OUTER RING: ZIRCATEC BUNDLE



OUTER RING: GEC BUNDLE

FIGURE 4
MEASUREMENTS VS PREDICTIONS OF COMPONENTS OF BUNDLE STIFFNESS

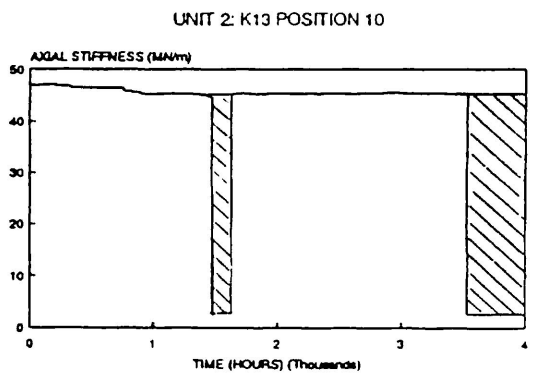
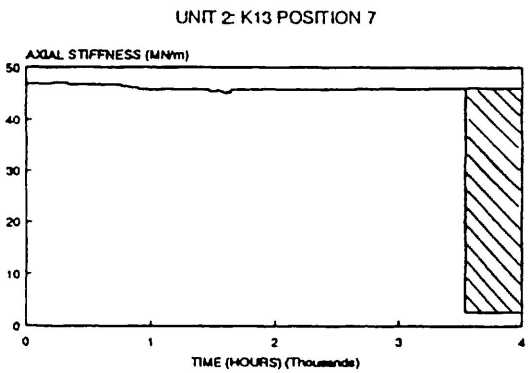
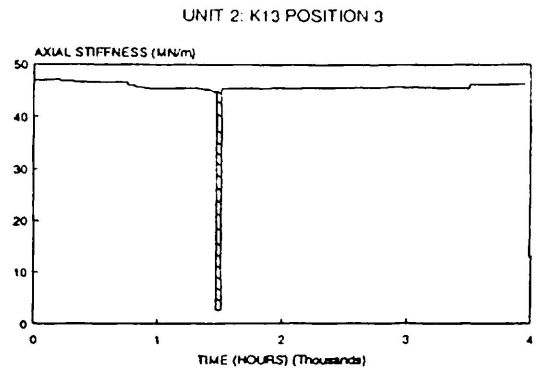
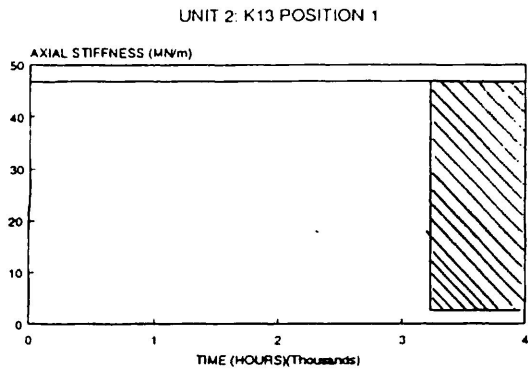
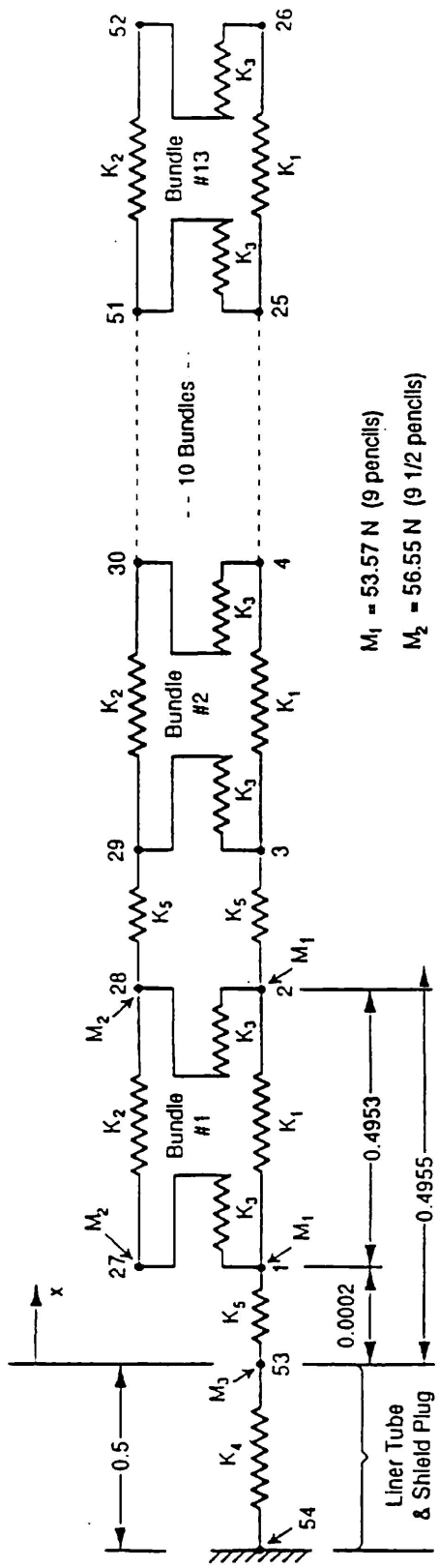


Figure 5

Calculated Outer Element Axial Stiffness Histories
for Bundles in Unit 2 Channel K13



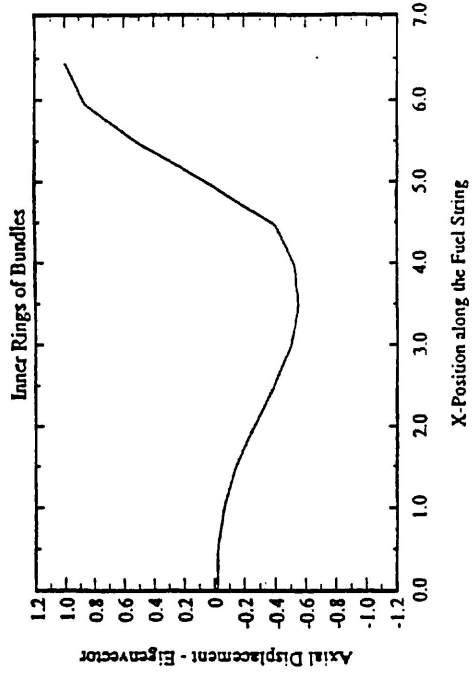
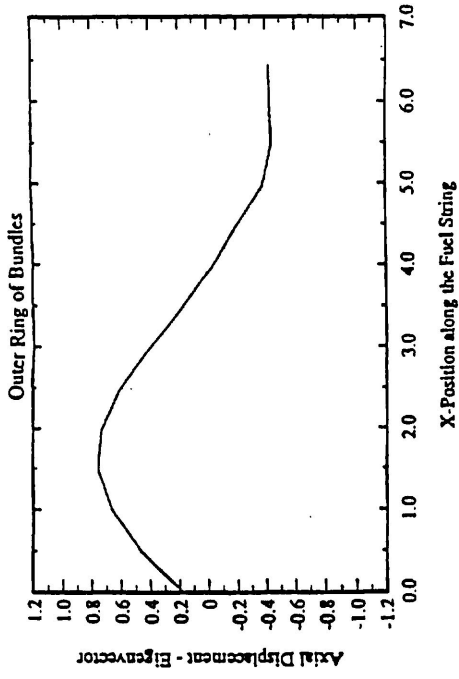
$M_1 = 53.57 \text{ N (9 pencils)}$
 $M_2 = 56.55 \text{ N (9 1/2 pencils)}$
 $M_3 = 756.16 \text{ N}$

$K_3 = 1.385 \text{ MN/m}$
 $K_4 = 112.1 \text{ MN/m}$
 $K_5 = 10000 \text{ MN/m}$

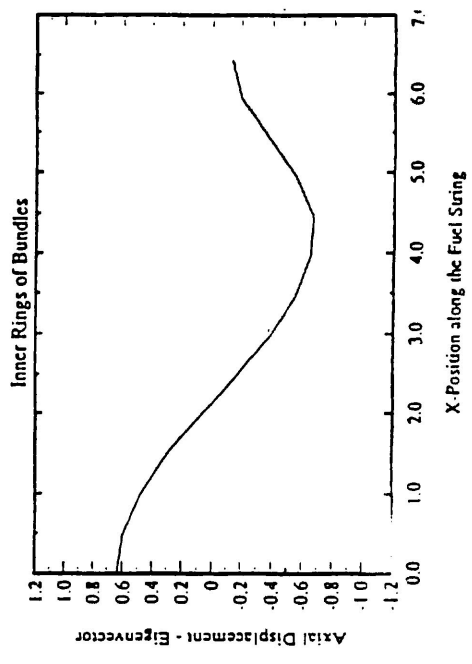
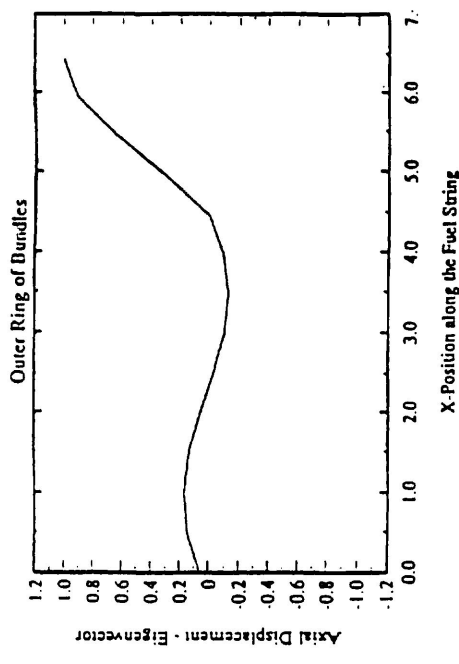
Note:

All Dimensions in meters

Figure 6
Uniaxial Fuel String Model



a) Mode 4: $f = 121$ Hz



b) Mode 5: $f = 139$ Hz

Figure 7

Analytical Mode Shapes of Fuel String - Modes 4 & 5

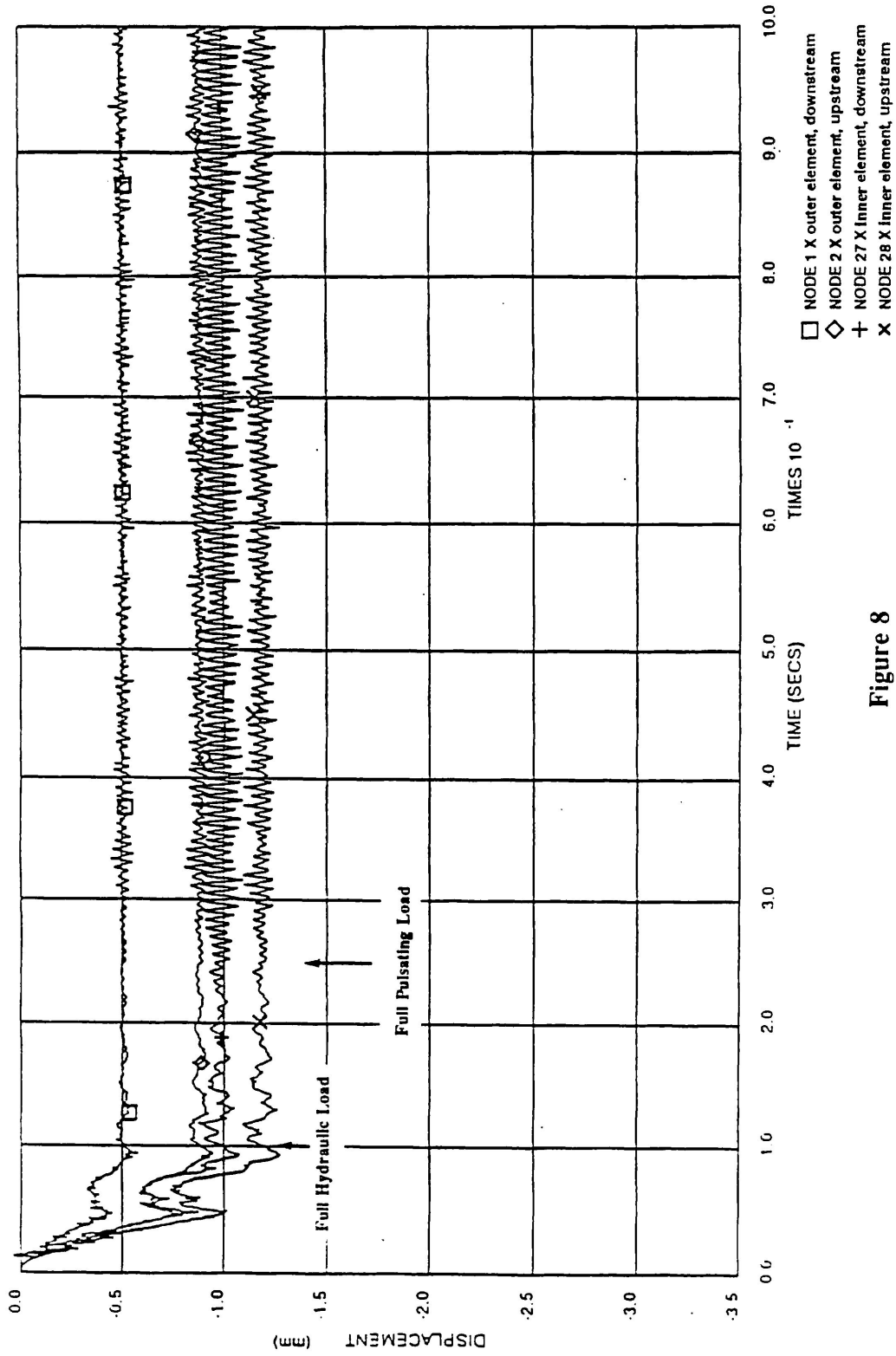


Figure 8

Bundle 1 Nodal Displacement Versus Time

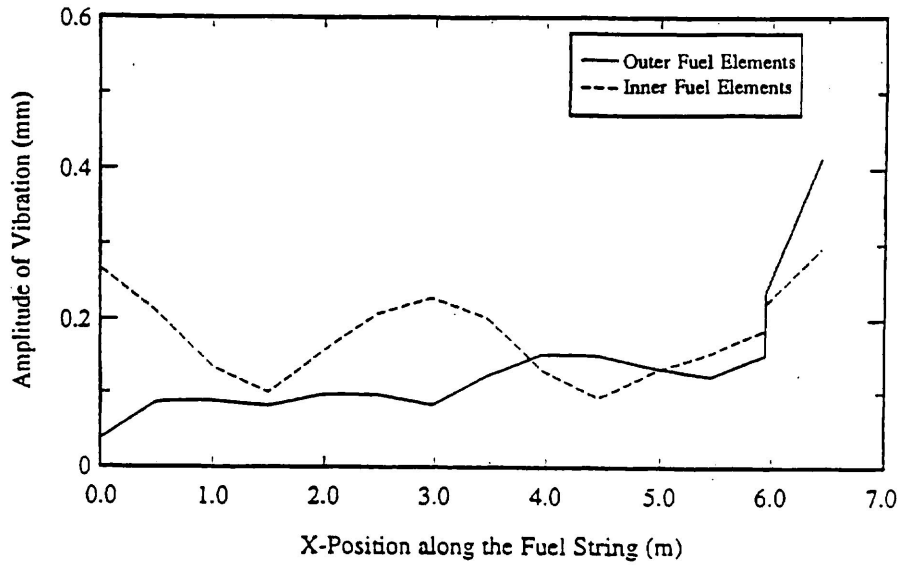


Figure 9a

Maximum Amplitude of Vibration due to 139 Hz Standing Wave

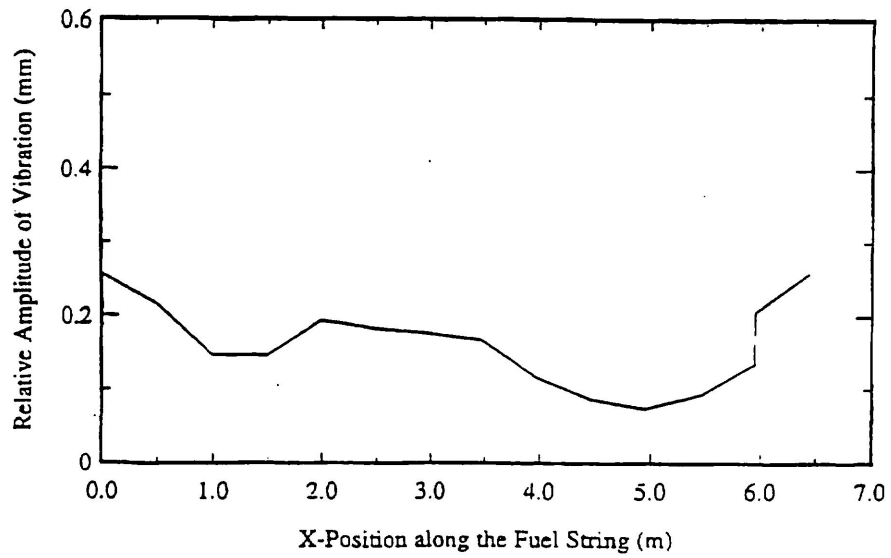


Figure 9b

Relative Amplitude of Vibration between Inner and Outer Fuel Elements due to a 139 Hz Standing Wave

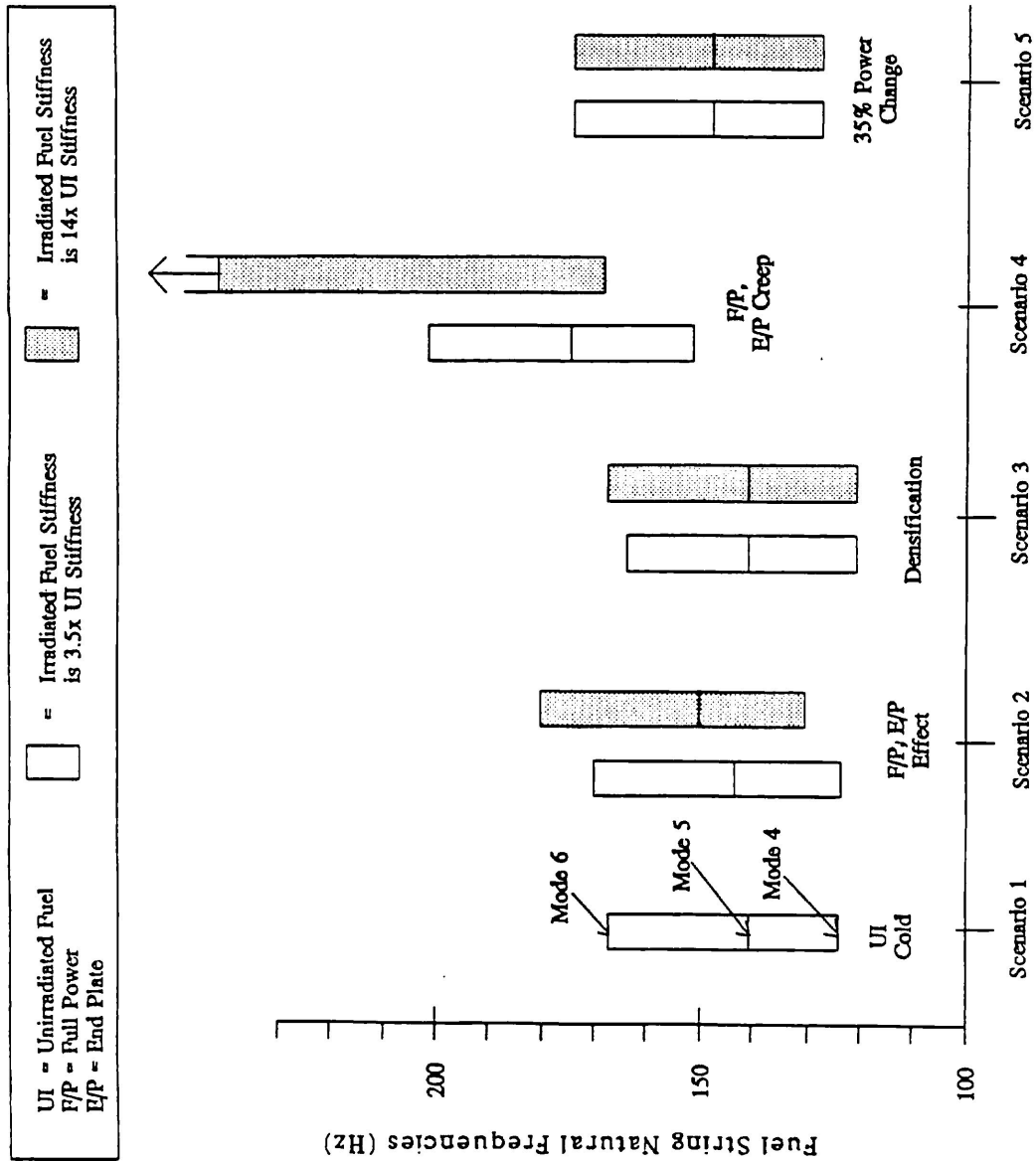


Figure 10

Calculated Natural Frequencies of the Fuel String Under Various Scenarios

